Hydration and Lateral Organization in Phospholipid Bilayers Containing Sphingomyelin: A ^{2}H-NMR Study

Bernhard Steinbauer, Thomas Mehnert, and Klaus Beyer
Lehrstuhl für Stoffwechselbiochemie der Universität München, Munich, Germany

ABSTRACT Interfacial properties of lipid bilayers were studied by ^{2}H nuclear magnetic resonance spectroscopy, with emphasis on a comparison between phosphatidylcholine and sphingomyelin. Spectral resolution and sensitivity was improved by macroscopic membrane alignment. The motionally averaged quadrupolar interaction of interlamellar deuterium oxide was employed to probe the interfacial polarity of the membranes. The D_2O quadrupolar splittings indicated that the sphingomyelin lipid-water interface is less polar above the phase transition temperature T_m than below T_m. The opposite behavior was found in phosphatidylcholine bilayers. Macroscopically aligned sphingomyelin bilayers also furnished ^{2}H-signals from the amide residue and from the hydroxyl group of the sphingosine moiety. The rate of water-hydroxyl deuteron exchange could be measured, whereas the exchange of the amide deuteron was too slow for the inversion-transfer technique employed, suggesting that the amide residue is involved in intermolecular hydrogen bonding. Order parameter profiles in mixtures of sphingomyelin and chain-perdeuterated phosphatidylcholine revealed an ordering effect as a result of the highly saturated chains of the sphingolipids. The temperature dependence of the ^{2}H quadrupolar splittings was indicative of lateral phase separation in the mixed systems. The results are discussed with regard to interfacial structure and lateral organization in sphingomyelin-containing biomembranes.

INTRODUCTION

Phosphatidylcholines and sphingomyelins are major constituents of cellular and subcellular bilayer membranes. Phosphatidylcholine is the dominant phospholipid species in most mammalian tissues whereas the sphingomyelin content varies considerably (Yorek, 1993). A large proportion of sphingomyelin is found in the outer leaflet of eukaryotic plasma membranes where it amounts to ~25% of the total phospholipid in humans and up to 50% in ruminants (Florin-Christensen et al., 2001). The sphingomyelin content is also high in the central nervous system and in the spinal cord. Of particular interest is the observation that the sphingomyelin content increases with age both in the cerebral cortex and in white matter where it reaches 18% of the total phospholipid (Nyberg et al., 1998; Yorek, 1993).

Phosphatidylcholine and sphingomyelin both have phosphocholine headgroups. There are, however, significant differences considering the properties of the interfacial and nonpolar segments of the molecules. Sphingomyelin has only one fatty acid in an amide linkage while the second hydrophobic chain is part of the sphingosine base structure whose interfacial part includes a hydroxyl group at C-3 and a *trans* double bound between C-4 and C-5 (Scheme 1). The amide plane in sphingolipids was shown to be roughly perpendicular with respect to the average orientation of the hydrophobic chains (Miller et al., 1986; Pascher, 1976; Ruocco et al., 1996).

The interfacial hydroxyl and amide residues of the sphingomyelin molecule are capable of donating and accepting hydrogen bonds while the carbonyl group of the N-acyl chain and the headgroup phosphodiester moiety may act as weak hydrogen bond acceptors. In contrast, there are only hydrogen bond acceptors in the interface of phosphatidylcholines; for example, the fatty acid carbonyls in *sn*-1 and *sn*-2 position of the glycerol backbone and the headgroup phosphate. It is tempting to assume that sphingomyelin interacts with itself and with surrounding phosphatidylcholine molecules by forming a network of hydrogen bonds. The amide linkage resides in a region of low dielectric constant, according to available structural data on ceramides (Pascher, 1976) and cerebrosides (Ruocco et al., 1996) which further promotes the formation of strong hydrogen bonds (Barenholz, 1984). This is in line with the low permeability of sphingomyelin bilayers for water and glucose (Hertz and Barenholz, 1975) and with ^{1}H-NMR relaxation time measurements (Schmidt et al., 1977). Similarly, monolayer surface compressional moduli (at a surface pressure of 30mN/m) are indicative of the tighter interfacial packing of sphingomyelins in comparison with chain-matched phosphatidylcholines (Li et al., 2001).

Infrared and Raman spectroscopy was applied to elucidate these structural properties in more detail. However, the results were not conclusive, e.g., it seems unclear whether intra- or intermolecular hydrogen bonds are responsible for the shifts in the amide I and II bands (Hübner and Blume, 1998; Lamba et al., 1991; Villalain et al., 1988). A number of high resolution ^{1}H- and ^{31}P-NMR studies in chloroform

Submitted November 27, 2002, and accepted for publication April 21, 2003.

Address reprint requests to Dr. Klaus Beyer, Lehrstuhl für Stoffwechselbiochemie der Universität München, Schillerstr. 44, 80336 München, Germany. Tel.: 49-89-599-6470; Fax: 49-89-599-6415; E-mail: kbeyer@med.uni-muenchen.de.

Abbreviations used: BBSM, bovine brain sphingomyelin; EYSM, egg yolk sphingomyelin; POPC, 1-palmitoyl-2-oleoyl-*sn*-glycero-3-phosphocholine; DPPC, 1,2-dipalmitoyl-*sn*-glycero-3-phosphocholine.

© 2003 by the Biophysical Society

0006-3495/03/08/1013/12 $2.00

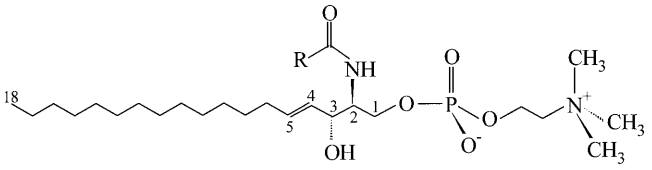

SCHEME 1

solution suggested an intramolecular hydrogen bond between the sphingosine OH group and the phosphodiester moiety of the choline headgroup (Bruzik, 1988; Talbott et al., 2000), in agreement with dynamic differences between the headgroups of phosphatidylcholine and sphingomyelin shown by ^{14}N-NMR spectroscopy (Siminovitch and Jeffrey, 1981).

The transition temperatures T_m of naturally occurring sphingomyelins are close to 37°C (Calhoun and Shipley, 1979) which may result in nonideal mixing and lateral separation of membrane domains under physiological conditions. The involvement of sphingolipids and cholesterol in membrane domains (''rafts'') has been demonstrated (London and Brown, 2000) and the significance for cell signaling and endocytosis is now generally accepted (Anderson and Jacobson, 2002). Sphingolipid binding domains have been recently identified in the amyloid peptide Aβ and in prion and HIV1 proteins (Mahfoud et al., 2002). These findings may be related to a recent report where it was shown that the level of sphingomyelin is increased in the brain of Alzheimer's disease patients (Pettegrew et al., 2001). Further, a relationship was found between the formation of the scrapie prion protein and the sphingomyelin content in neuroblastoma cells (Naslavsky et al., 1999). Thus, an investigation of the properties of the sphingomyelin-water interface is of considerable biomedical interest.

The present study provides a comparison of phosphatidylcholines and sphingomyelins and of mixtures of both lipids with emphasis on interfacial hydration and hydrogen bonding in the vicinity of phase transitions. The role of cholesterol in these systems is beyond the scope of the present work and will be addressed in a later communication. Macroscopically aligned multibilayers were employed (Kurze et al., 2000) and the hydration was kept at or slightly below what is generally considered as ''fully hydrated.'' This technique avoids problems associated with the heterogeneity of random multibilayer systems (König et al., 1997b; Nagle et al., 1999) and yields maximum sensitivity and resolution. Our results suggest that the fraction of water associated with polar groups in the lipid interface decreases with increasing mole fraction of sphingomyelin in the bilayer.

MATERIALS AND METHODS

Chemicals

Synthetic phospholipids (POPC, POPC-d_{31}, DPPC, DPPC-d_{62}, and α,β-d_4-DPPC) were obtained from Avanti Polar Lipids (Alabaster, AL). Sphingolipids (EYSM and BBSM) were also from Avanti or from Sigma-Aldrich (Deisenhofen, Germany). Deuterated solvents were purchased from Cambridge Isotope Laboratories (Promochem GmbH, Wesel, Germany). The lipids were checked for purity by thin layer chromatography before and after NMR measurements.

Sample preparation

Macroscopically aligned phospholipid multibilayers were prepared as described previously (Kurze et al., 2000). Briefly, 30 mg of the lipid or lipid mixture were dissolved in 5 ml of methanol or deuterated methanol (CH_3OD). The latter was required when complete exchange of labile protons in sphingomyelins was desirable. The solutions were spread onto 50 ultrathin glass plates (8 × 18 × 0.08 mm; Marienfeld Lab. Glassware, Lauda-Königshofen, Germany) and dried for 20 min under a stream of warm air and then at room temperature for at least 18 h in vacuo (20–30 Pa). The glass plates were stacked on top of each other with gentle pressure and inserted, along with a pair of glass cylinder segments, into an open glass tube (inner diameter 9.8 mm; compare to Fig. 1 in Kurze et al., 2000). Two small paper strips were soaked in D_2O and carefully dried to exchange labile hydrogen for deuterium. The strips were attached at the short sides of the glass stacks and a few microliters of D_2O were applied onto the paper surface. The tube was rapidly stoppered by two appropriately machined Teflon plugs with silicon O-rings. The membranes were annealed for 8 h at 46°C in the probehead and the annealing process was continuously monitored by ^{2}H-NMR spectroscopy. The hydration step was repeated until the desired hydration was achieved. During long-term acquisitions the tubes were wrapped with parafilm to maintain the hydration level. With this precaution, no changes of the hydration level were observed at 42°C within 5 h. (For further details of the alignment technique, see Kurze et al., 2000.)

^{2}H-NMR

^{2}H-NMR spectra were recorded using a Varian VXR-400 spectrometer operating at 9.4 T (^{2}H-frequency 61.4 MHz). Spectra of macroscopically

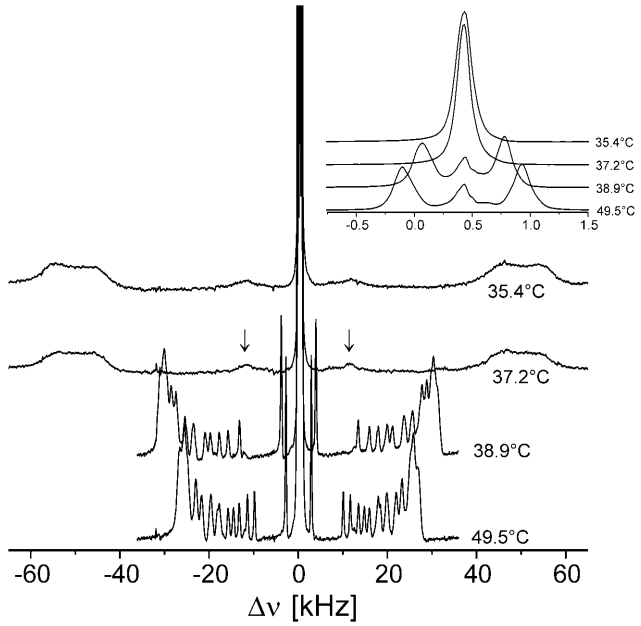

FIGURE 1 ^{2}H-NMR spectra of macroscopically aligned multibilayers of DPPC-d_{62}, recorded in the vicinity of the phase transition temperature. (*Arrows*) Terminal methyl ^{2}H resonances. The bilayers were hydrated with D_2O (n_w = 23). The corresponding ^{2}H spectra of interlamellar D_2O are shown in the inset.

aligned samples were acquired using a 10-mm flat wire solenoid. A home-built goniometer, driven by a stepper motor under software control, was used for accurate orientation in the magnetic field at $\theta = 0°$ where θ denotes the angle between the normal to the bilayer stack with respect to the field direction (Kurze et al., 2000). Order parameters for individual carbon positions in the *sn*-1 chain of POPC-d_{31}were obtained according to

$$\Delta\nu_Q^{(i)} = \frac{3}{2}\chi P_2(\cos\Theta)|S_{CD}^{(i)}|, \quad (1)$$

where χ denotes the quadrupolar coupling constant (170 kHz for a CD bond), $P_2(\cos\Theta)$ the second Legendre polynomial, and $S_{CD}^{(i)}$ the order parameter of the i^{th} carbon-deuterium bond in the hydrocarbon chain. The quadrupolar echo sequence (Davis et al., 1976) was applied for signal excitation using composite pulses with a 90° pulse width of 7 μs and a pulse spacing of 20 μs. The number of water molecules per lipid headgroup (n_w) was obtained by calculating the integral ratio of the respective ^{2}H signals from D_2O and from permanently (α,β-d_4-DPPC, POPC-d_{31}) or exchange-labeled (EYSM, BBSM) lipids. Integration of the upfield and downfield regions of the ^{2}H NMR spectra, after careful phase adjustment, yielded an estimated error in water content of $\delta n_w \leq 0.5$. The recycle delays were chosen so as to avoid saturation.

The rate constants of labile deuteron exchange were determined using the inversion-transfer technique (Led and Gesmar, 1982). The D_2O doublet was selectively inverted using a low-power radiofrequency pulse at the center frequency in the spectrum (90° pulse width, 140 μs). The entire inversion-transfer sequence was π_{sel}-Δ-$\pi/2_x$-τ-$\pi/2_y$-τ-acquisition, where the selective 180° pulse, π_{sel}, inverts the D_2O signal, and the nonselective 90° pulses, $\pi/2$, represent the usual quadrupolar echo sequence. Increasing the delay Δ then results in the expected time variation of those signals that correspond to rapidly exchanging labile deuterons in the lipid interface (compare to Fig. 6). Reference spectra were recorded after each acquisition in the inversion transfer series and signal amplitudes were normalized with respect to the average amplitudes in the reference spectra. The D_2O signal was suppressed after signal acquisition by digital filtering (low frequency signal suppression) to minimize baseline distortions and integration artifacts at the OD resonance positions. Thirty five filter coefficients were employed for a sharp filter cutoff (VNMR software, version 5.1). Inversion recovery experiments, i.e., π_{nonsel}-δ-$\pi/2_x$-τ-$\pi/2_y$-τ-acquisition, were performed immediately after the inversion transfer series to obtain the spin lattice relaxation time T_{1z} for the interbilayer D_2O which was assumed to be independent of the deuteron exchange rate. Nine δ-increments and 64 transients per increment were sufficient for a reliable T_{1z} determination.

The inversion transfer results were evaluated on the basis of coupled differential equations for a two-side exchange (Led and Gesmar, 1982), e.g., for a deuteron in a hydroxyl group:

$$\frac{dM^{OD}}{dt} = k_W M^W - k_{OD} M^{OD} - (M^{OD} - M_\infty^{OD})R_{1OD} \quad (2)$$

$$\frac{dM^W}{dt} = -k_W M^W + k_{OD} M^{OD} - (M^W - M_\infty^W)R_{1W}, \quad (3)$$

where M^{OD}, M^W, M_∞^{OD}, and M_∞^W denote the magnetizations and the equilibrium magnetizations, and R_{1OD}, R_{1W} the longitudinal relaxation rates of the OD and water deuterons, respectively. The exchange rate constants k_{OD} and k_W refer to the deuteron transfer from D_2O to the hydroxyl group in the sphingosine moiety and vice versa. A further condition is provided by the chemical equilibrium, i.e.,

$$k_W M_\infty^W = k_{OD} M_\infty^{OD}. \quad (4)$$

The results were numerically evaluated as described previously (Kurze et al., 2000).

Differential scanning calorimetry

Measurements were performed using a VP-DSC instrument (Microcal, Northhampton, MA). Scan rates were typically 15°C/h.

RESULTS

Hydration of phosphatidylcholine and sphingomyelin bilayers

Macroscopic alignment of phospholipid membranes has distinct advantages for ^{2}H-NMR spectroscopy, including improved spectral resolution, hydration of the membranes under strict experimental control, and excellent sensitivity for phase transitions. This is shown in Fig. 1 for multibilayers of chain-perdeuterated 1,2-dipalmitoyl-*sn*-glycero-3-phosphocholine (DPPC-d_{62}). The membranes were hydrated with D_2O as described in the Methods section and the supporting glass plates were oriented so as to obtain the maximum quadrupolar splittings, indicating that the normal to the membrane surface was parallel to the magnetic field ($\Theta = 0°$, compare to Eq. 1). Before data acquisition the hydration level, typically starting from 30 mol of D_2O per mole of phospholipid ($n_w = 30$), was adjusted by slow water evaporation in the magnet to $n_w = 24$ as determined by signal integration. The spectra were recorded at a number of temperatures, including the temperature T_m of the phospholipid main phase transition. Upon cooling from the liquid crystalline state a sudden increase of the ^{2}H line widths and quadrupolar splittings of the deuterated hydrocarbon chains is observed ~38°C which is close to the transition temperature (37.75°C) reported earlier for DPPC-d_{62} in excess water (Vist and Davis, 1990), indicating that the multibilayer system can be considered as ''fully hydrated.''

The quadrupolar splittings of the interlamellar deuterium oxide ($\Delta\nu_Q^{D_2O}$) vanishes as the temperature reaches T_m, in contrast to the splittings of the phospholipid acyl chains (*inset*, Fig. 1). This is also shown in Fig. 2, where $\Delta\nu_Q^{D_2O}$ is plotted versus the *reduced* temperature; for example, $(T - T_m)/T_m$. Fig. 2 includes data from 1-palmitoyl-2-oleoyl-*sn*-glycero-3-phosphocholine (POPC). In the liquid crystalline state $\Delta\nu_Q^{D_2O}$ decreases monotonically with decreasing reduced temperature for both phospholipids at full hydration ($n_w \approx 24$). There is a unique dependence of $\Delta\nu_Q^{D_2O}$ with reference to the reduced temperature although the phase transition temperatures, T_m differ significantly (41°C *vs.* −5°C for DPPC and POPC, respectively). This homology suggests that the accessibility of polar groups for the interlamellar D_2O molecules is very similar in the liquid crystalline state of these lipids.

The alignment technique was further employed to explore the interfacial properties of sphingomyelin multibilayers in the vicinity of the phase transition temperature. Natural species from two different sources were analyzed: sphingomyelin from egg yolk (EYSM) and from bovine brain (BBSM). The sphingomyelin samples were first dissolved in

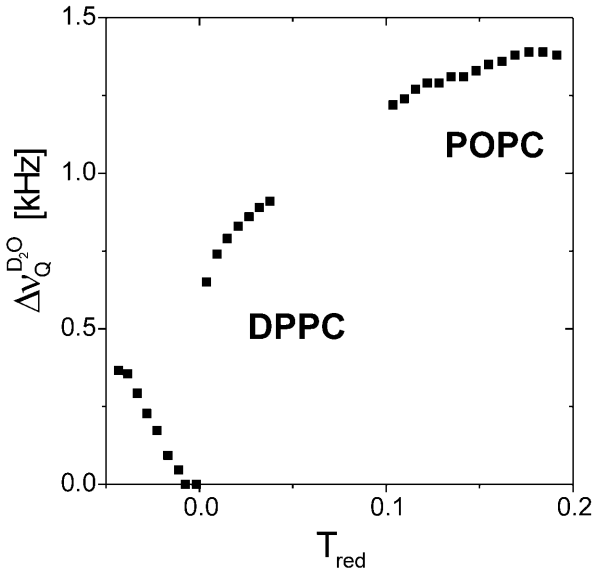

FIGURE 2 ^{2}H quadrupolar splittings of interlamellar D_2O in multibilayers of DPPC and POPC as a function of the reduced temperature, $T_{red} = (T - T_m)/T_m$, where T denotes temperatures in K.

the presence of deuterated methanol (CH_3OD) before spreading the lipid onto glass plates. This procedure results in complete exchange of the labile hydrogens of the hydroxyl group at C-3 and of the amide residue at C-2 of the sphingosine base by deuterium. ^{2}H-NMR spectra obtained from oriented EYSM multibilayers ($n_w = 32$) are shown in Fig. 3 *A* where the strong signal from interlamellar D_2O has been removed by digital filtering to show more clearly the weak OD and ND resonances. The observation of these signals in the liquid crystalline state of the lipid indicates that chemical exchange among hydroxyl and amide deuterons, as well as exchange with the interlamellar water, is slow on the NMR timescale.

The assignment of the signals relies on the assumption that rapid rotation of the hydroxyl deuteron about the C=O bond

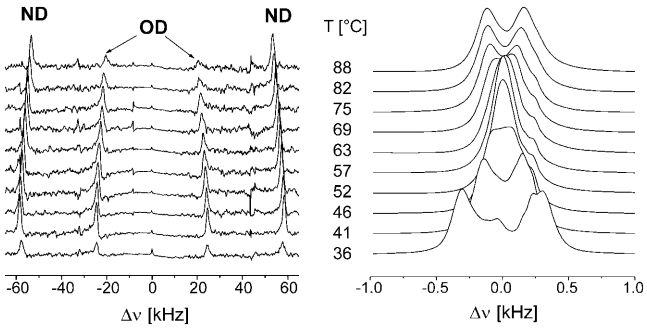

FIGURE 3 Temperature dependence of ^{2}H-NMR spectra of exchange-labeled EYSM multibilayers. (*Left panel*) ^{2}H doublets of the hydroxyl and amide residues in the sphingosine backbone. The large D_2O doublet signals in the center of the spectra were removed by digital filtering. (*Right panel*) The corresponding signals from interlamellar D_2O ($n_w \approx 32$).

reduces the OD quadrupolar splitting, i.e., the effective splitting corresponds to the projection of the OD vector onto the C-O axis. Further, it has been shown by ^{13}C solid-state NMR spectroscopy that the amide plane is inclined by 35°–52° with respect to the bilayer surface (Ruocco et al., 1996). This would be consistent with an orientation of the N-D bond axis nearly parallel to the membrane surface or, in the present experiment, perpendicular to the magnetic field. Using a typical value for the quadrupolar coupling constant, $\chi = 240$ kHz, for hydrogen bonded amide deuterons in gramicidin A (Prosser et al., 1994), a rigid perpendicular orientation would result in a quadrupolar splitting of 180 kHz. The values obtained experimentally are smaller than this (*e.g.*, 117 kHz at 41°C; see Fig. 3), which may account for motional averaging in the membrane interface as compared to the rigid membrane-bound peptide. Unfortunately, χ strongly depends on the hydrogen bond length, which makes an estimate of quadrupolar splittings uncertain, even if one assumes a rigid perpendicular bond orientation. The quadrupolar splittings of the outer and inner doublet signals decrease between 41°C and 88°C by 8.7% and 16.3%, respectively, which can be attributed to enhanced bilayer fluctuation.

A remarkable feature in Fig. 3 is the temperature dependence of the ^{2}H line widths—i.e., there is a significant broadening of the inner, but not of the outer, doublet components in the high temperature region ($T > 70$°C). Given the above signal assignment, this differential broadening most probably indicates that chemical exchange of the hydroxyl deuteron with deuterons from interfacial water is more effective than the exchange of the amide deuteron. Below 40°C the amplitudes of *both* signals decrease simultaneously, which is most likely due to line broadening when the lipid enters the gel state. Eventually, <30°C the signals are no longer detectable.

The spectral features in Fig. 3 are correlated with the phase transition as detected by differential scanning calorimetry (DSC; Fig. 4). The temperature dependence of the signal amplitudes of the ND and OD resonances (normalized with respect to the signal amplitudes obtained above T_m) are shown as solid symbols while the solid lines represent normalized integrals of the heat capacity obtained by DSC, i.e., $\int_{T_{min}}^{T} C_P(T')dT' / \int_{T_{min}}^{T_{max}} C_P(T')dT'$. The almost perfect agreement between this data indicates that the ^{2}H signal amplitudes sense the phase transition with great accuracy. The transition is broader for BBSM than for EYSM, which can be attributed to the greater heterogeneity of the fatty acid composition of the former sphingomyelin species.

The splittings $\Delta\nu_Q^{D_2O}$ of the D_2O signal (that has been removed in Fig. 3, *left panel*) are also related to the phase transition (*open symbols* in Fig. 4). Close to the transition temperature, $\Delta\nu_Q^{D_2O}$ runs through an inflection point for EYSM and through a minimum for BBSM, respectively. In the EYSM sample there is also a minimum ~51°C, i.e., ≈13°C above the phase transition temperature (≈38°C). Notably, $\Delta\nu_Q^{D_2O}$ is rather small or zero in the liquid

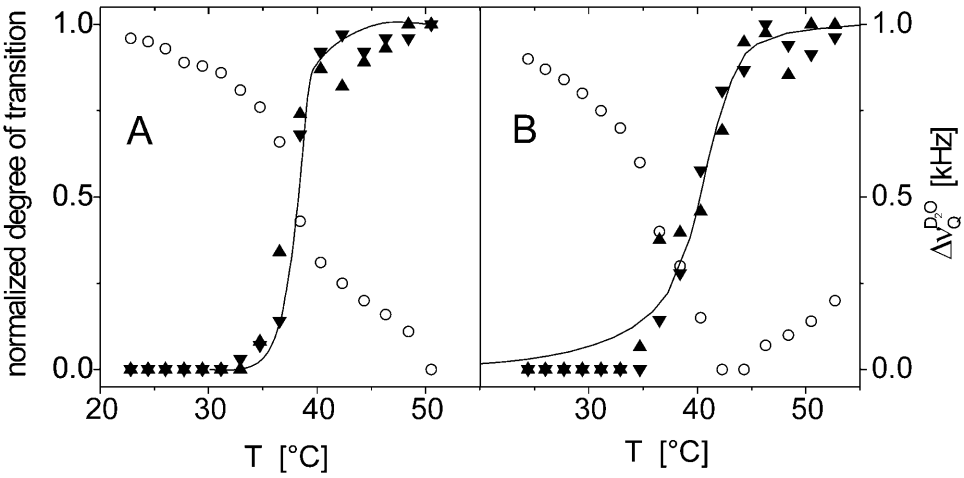

FIGURE 4 The phase transition of (*A*) fully hydrated EYSM ($n_w \approx 32$) and (*B*) BBSM ($n_w \approx 41$) as detected by ^{2}H NMR in aligned multibilayers and by DSC (multilamellar vesicles). Normalized signal amplitudes (*solid symbols*), $I(t)/I_{max}$, of ND (▲) and OD (▼) resonances, where I_{max} denotes the amplitudes in the liquid crystalline state. Degree of phase transition obtained by DSC (*solid lines*). (○) Quadrupolar splittings of interlamellar D_2O.

crystalline state of the sphingolipids, in contrast to lecithin bilayers (compare to Fig. 2). Fig. 5 summarizes the temperature dependence of the water splittings obtained at similar hydration for EYSM and DPPC alone and for a EYSM/DPPC mixtures at 2:1 and 1:1 molar ratios. Obviously, sphingomyelin controls the properties of the lipid-water interface in the mixed systems.

Interfacial deuteron exchange

The chemical exchange of labile deuterons (i.e., the hydroxyl and amid deuterons) was measured as described previously, using an inversion-transfer technique (Kurze et al., 2000). This involves inversion of the D_2O signal in the center of the spectrum by a frequency selective low power pulse followed by a variable delay time Δ and a nonselective quadrupolar echo sequence for excitation of the entire spectrum. Magnetization transfer then results in variation of the signal amplitudes of those labile lipid deuterons that exchange with the surrounding water at a rate larger than the spin lattice relaxation rate $1/T_{1z}$.

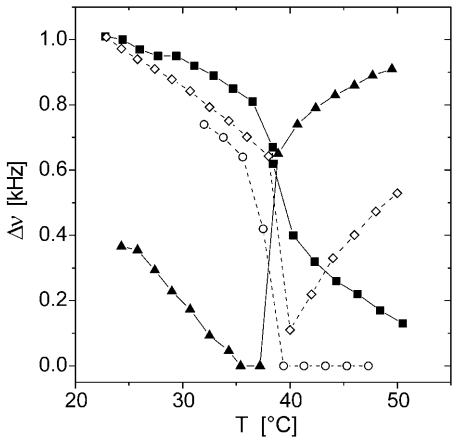

FIGURE 5 Comparison of the D_2O quadrupolar splittings in the vicinity of the phase transition temperature for DPPC (▲), EYSM (■), and EYSM/DPPC mixtures at 2:1 (○) and 1:1 (◇) molar ratio. Hydration $n_w \approx 25$.

Fig. 6, *A* and *B*, show a series of ^{2}H-NMR spectra of aligned EYSM multibilayers ($n_w = 29$) recorded with increasing delay time Δ and the evaluation of the magnetization transfer according to Eqs. 2–4 (see Methods). Again, the central D_2O signal was digitally filtered to facilitate observation of the OD and ND signals. The doublet that has been attributed to the sphingosine OD residue varies with increasing Δ whereas the amplitudes of the ND resonances hardly change within the time course of the experiment, indicating that the amide deuteron exchange rate is much smaller than the exchange rate of the hydroxyl deuteron. This result is in qualitative agreement with the temperature dependence of the ^{2}H line broadening shown in Fig. 3.

The rate constant k_{OD} increases with increasing temperature (Fig. 6 *C*). For EYSM ($n_w = 26$), k_{OD} was 387 ± 65 s^{-1} at 39°C (close to the phase transition temperature) and 1000 ± 75 s^{-1} at 55°C. The rather large exchange rate obtained at 55°C is comparable to the rate of proton exchange in pure water (1100 s^{-1} at 25°C, pH = 7) (Luz and Meiboom, 1964) which argues against strong intermolecular hydrogen bonding of the EYSM hydroxyl group. In contrast, the amide hydrogen seems to be protected from exchange with the interlamellar water. The exchange rate constants at slightly different hydration values follow the same trend (Fig. 6 *C*) which justifies an evaluation in terms of a single activation energy. Only data for $n_w \geq 20$ were included in the analysis as membranes at lower hydration values certainly cannot be considered as ''fully hydrated.'' Linear regression of the entire data set yields an average activation energy of 41 ± 6kJ/mole which is considerably larger than the activation energies reported for proton exchange in pure water (see Discussion).

The exchange rate constants also increased as a function of n_w; e.g., for EYSM, at 47°C from 350 ± 20 s^{-1} to 750 ± 90 s^{-1} ongoing from $n_w = 17$ to $n_w = 29$ (data not shown). Unfortunately, a determination of k_{OD} at lower hydration

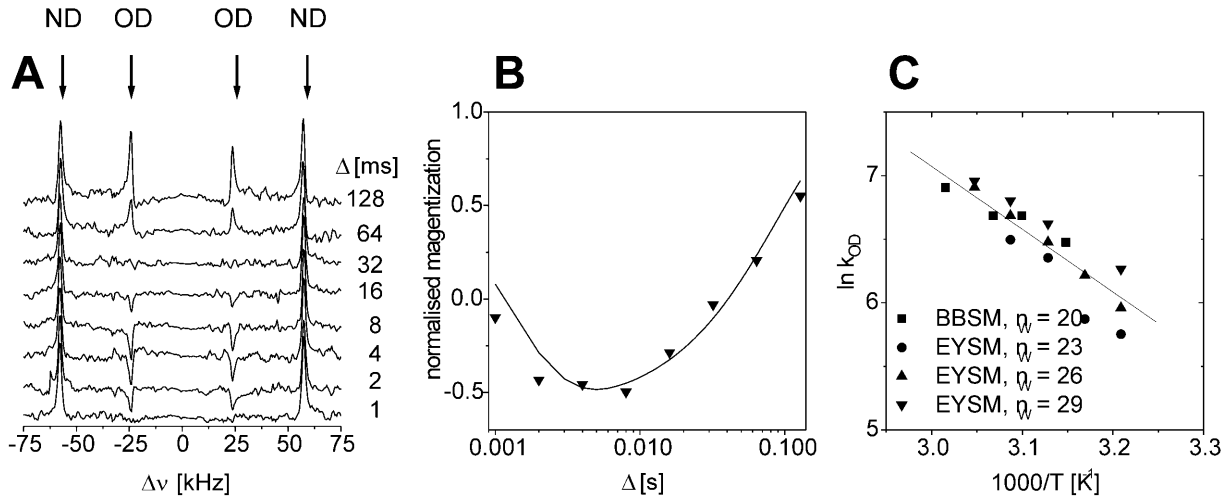

FIGURE 6 Determination of deuteron exchange in the sphingomyelin-water interface (42°C, $n_w \approx 29$). (*A*) Typical inversion recovery series of ^{2}H spectra obtained by the pulse sequence π_{sel}-Δ-$\pi/2_x$-τ-$\pi/2_y$-τ-acquisition. (*B*) Variation of the OD signal amplitude with delay time Δ. (*C*) Arrhenius representation of the temperature dependence of the deuteron exchange rate k_{OD}.

values was not feasible as additional D_2O signals with unusually large quadrupolar splittings appeared $<n_w \approx 15$ in pure SM multibilayers, e.g., three signal components could be identified at 47°C at $n_w = 12$. Moreover, the ND and OD signals were no longer detectable, indicating that the phase transition temperature T_m increased >10°C due to dehydration of the membrane interface. A very broad, temperature-dependent component of the water signal persisted above T_m, reaching a quadrupolar splitting $\Delta\nu > 10$ kHz at 57°C (data not shown). Thus, an interpretation of exchange data would be impossible even if inversion of the water magnetization had been achieved.

Binary sphingomyelin/phosphatidylcholine mixtures

Binary mixtures of BBSM and *sn*-1-d_{31}-palmitoyl-*sn*-2-oleoyl-glycero-3-phosphocholine (POPC-d_{31}) were studied with regard to hydration, intermolecular packing, and phase transition, again using macroscopically oriented membrane multibilayers. BBSM was chosen here, as a comprehensive investigation of the system BBSM/egg lecithin/water has been published previously (Untracht and Shipley, 1977). Likewise, egg lecithin has a high amount of oleic acid in the *sn*-2 position and thus closely resembles POPC. Fig. 7 *A* summarizes the quadrupolar splittings of interlamellar D_2O at the same overall hydration ($n_w \approx 26$) obtained over a temperature range from 20°C to 50°C for pure POPC-d_{31} and for mixtures of BBSM and POPC-d_{31} at molar ratios 2:1 and 1:2, respectively. The splittings increase monotonously in this temperature range for POPC-d_{31} alone and for the mixture containing 33 mol % of BBSM, shown in Fig. 7 *A*, whereas in the presence of 67 mol % of BBSM, $\Delta\nu_Q^{D_2O}$ goes through a minimum at 30°C. The minimum can be attributed to a phase transition, in analogy to the results obtained with BBSM alone (Fig. 4). At 46°C, with increasing mole fraction of BBSM, the splittings decrease in a nonlinear fashion, which may reflect nonideal mixing of the system, even in the liquid crystalline state at some distance from the phase transition temperature (Fig. 7 *B*).

A characteristic feature of naturally occurring sphingomyelins is the high proportion of saturated long-chain fatty acids (Barenholz and Thompson, 1999). Deuterium order parameter profiles offer a direct proof of the effect of the sphingolipids on the overall packing density in mixed bilayers. Segmental ^{2}H order parameters of the *sn*-1 chain of POPC–d_{31} in sphingomyelin/POPC mixtures, normalized with respect to the corresponding order parameter values for POPC-d_{31} alone, are shown as a function of carbon position in Fig. 8. The signal assignments rely on the usual assumption that the order parameters decrease with increasing distance from the membrane-water interface. Quadrupolar splittings for carbon positions 2–8 were poorly resolved (the order parameter ''plateau'') and rather insensitive to the presence of the sphingolipids. Therefore, only resolved resonances are included in Fig. 8.

Addition of BBSM (BBSM/POPC-d_{31}, 2:1 mol/mole) leads to a remarkable increase of the normalized POPC-d_{31} order parameters in the middle of the bilayer, with a flat maximum around carbon position 14. Thus, addition of BBSM reduces the probability of chain isomerization which amounts to an increased average projected length of the POPC *sn*-1 chain as compared to a pure POPC bilayer (Salmon et al., 1987; Schindler and Seelig, 1975). The effect clearly increases with higher molar ratios of BBSM/POPC-d_{31}, i.e., the normalized ordering profile is lower at 1:2 than at 2:1 molar ratio, whereas the temperature dependence seems to be merely small. Interestingly, the flat maximum shifted toward the membrane-water interface when BBSM was replaced with EYSM (Fig. 8, *crosses* connected by

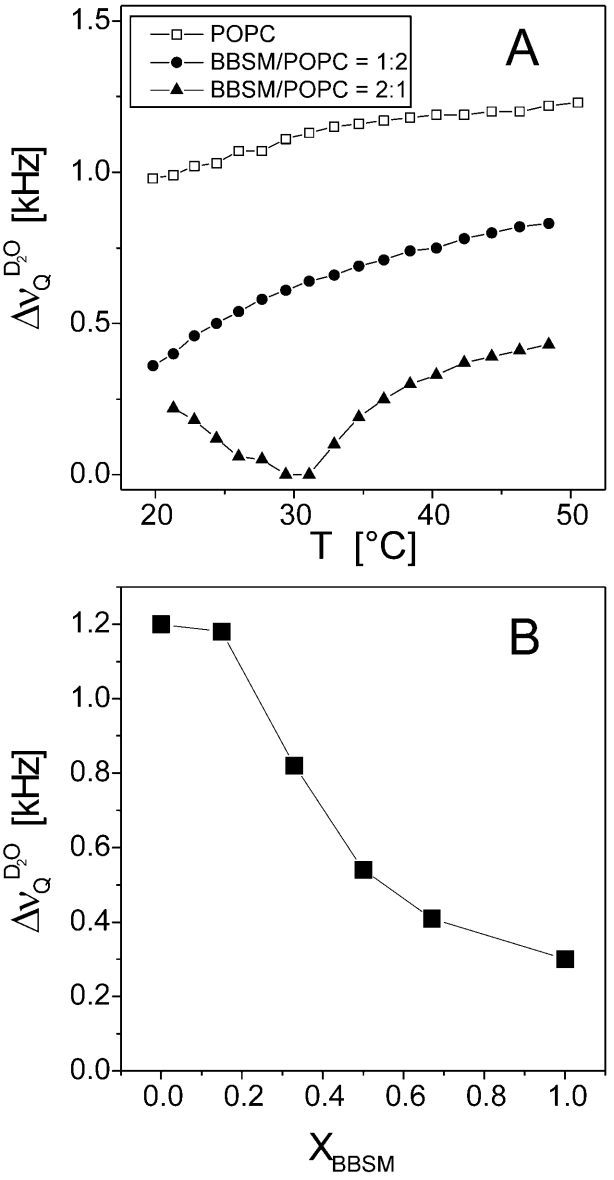

FIGURE 7 (*A*) Temperature dependence of the D_2O quadrupolar splittings in BBSM/POPC mixtures. (*B*) D_2O splitting as a function of the BBSM mole fraction at 46°C. Hydration, $n_w \approx 26$.

dashed lines), which must be attributed to the shorter acyl chain length in this sphingomyelin species (16:0, 83.9%; 18:0, 6.3%; other, 9.8% in EYSM *vs*. 18:0, 45.5%; 22:0, 7.2%; 24:0, 23.3%; and other, 14% in BBSM; Jendrasiak and Smith, 2001). An even larger increase of the POPC-d_{31} order parameters was observed when sphingomyelin was replaced with the synthetic phospholipid DPPC (order parameter ratio $\approx$ 1.3 at carbon 13 in a 2:1 DPPC/POPC-d_{31} mixture at 42°C, data not shown). It can be concluded that there is a condensing effect in mixed bilayers containing natural sphingomyelins due to the high abundance of saturated chains. It may also be argued that interfacial hydrogen bonding contributes to the closer lipid packing (Barenholz and Thompson, 1999).

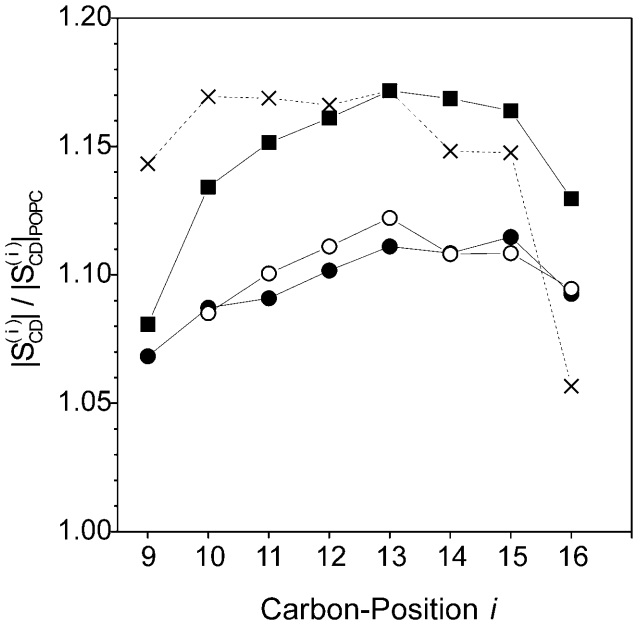

FIGURE 8 Order parameters of the POPC-d_{31} acyl chain in sphingomyelin/POPC mixtures, normalized with respect to the corresponding order parameters of POPC-d_{31} alone. (×) EYSM/POPC-d_{31}, 2:1 mol/mole, 42°C; (■) BBSM/POPC-d_{31}, 2:1 mol/mole, 42°C; (●) BBSM/POPC-d_{31}, 1:2 mol/mole, 42°C; and (○) BBSM/POPC-d_{31}, 1:2 mol/mole, 21°C.

The data in Fig. 8 correspond to virtually fully hydrated membranes ($n_w \approx 27$) in the liquid crystalline state where the components are completely miscible. Decreasing the interlamellar hydration shifts the phase transition toward higher temperatures and eventually results in lateral phase separation (Untracht and Shipley, 1977). One can expect that in the two-phase region the acyl chains of POPC will return to the more disordered state when sphingomyelin in the gel state separates from the mixture. This is shown in Fig. 9 *A* where the ^{2}H quadrupolar splittings of the terminal CD_3 residue, $\Delta\nu_Q^{CD_3}$, of the POPC-d_{31} *sn*-1 chain are plotted as a function of temperature for two different hydration values and three lipid compositions.

For POPC alone, $\Delta\nu_Q^{CD_3}$ decreases monotonously with increasing temperature, both at full ($n_w \approx 26$) and reduced ($n_w \approx 11$) hydration. Addition of BBSM, as expected from Fig. 8, increases the quadrupolar splitting, $\Delta\nu_Q^{CD_3}$, which is more pronounced when $n_w \approx 11$. Upon lowering the temperature, i.e., when the system approaches the phase transition from the liquid crystalline state, $\Delta\nu_Q^{CD_3}$, for the BBSM/POPC-d_{31} 2:1 mol/mole mixture, deviates toward the splittings obtained for pure POPC-d_{31}, most probably as a consequence of chain demixing. At low membrane hydration ($n_w \approx 11$) a slight inflection of the temperature dependence can be also recognized for the 1:2 mixture. A similar behavior was found for the ''plateau'' values, comprising the methylene deuterons from C-2 to C-7 of the *sn*-1 chain; i.e., the splittings reach a maximum at 39°C and approach the values observed for POPC-d_{31} alone ~20°C (data not

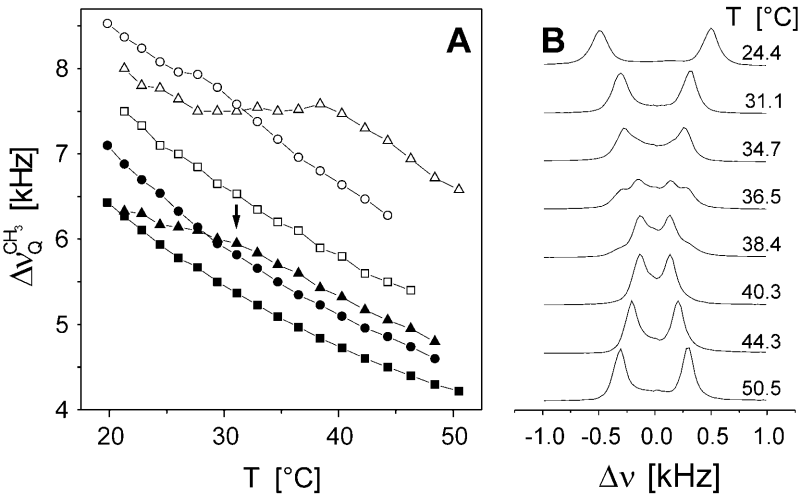

FIGURE 9 (*A*) Quadrupolar splittings of the ω-CD_3 group of POPC-d_{31} in mixed BBSM/POPC-d_{31} multibilayers. At $n_w \approx 26$: (■) POPC-d_{31} alone; (●) BBSM/POPC-d_{31}, 1:2 mol/mole; (▼) BBSM/POPC-d_{31}, 2:1 mol/mole; and at $n_w \approx 11$: (□) POPC-d_{31} alone; (○) BBSM/POPC-d_{31}, 1:2 mol/mole; (Δ) BBSM/POPC-d_{31}, 2:1 mol/mole. (*B*) ^{2}H spectra of interlamellar D_2O obtained in the BBSM/POPC-d_{31} mixture at $n_w \approx 11$ (2:1 mol/mole).

shown). Note that for $n_w \approx 26$ the breakpoint occurs at 31°C (*arrow* in Fig. 9 *A*), where $\Delta\nu_Q^{D_2O}$ goes through a minimum (compare to Fig. 7). Our results are in excellent agreement with the phase diagram obtained by Untracht and Shipley, which shows a broad two-phase region for a 2:1 mol/mole BBSM/egg lecithin mixture in the same temperature range at a hydration of $n_w \approx 11$ (Untracht and Shipley, 1977).

Lateral phase separation can also be recognized in the D_2O spectra at $n_w \approx 11$ (but not at hydration values $n_w > 20$). A broad second component that increases with decreasing temperature appears <40°C (Fig. 9 *B*). The narrow component of the composite spectra disappears <30°C. The coexistence of ^{2}H subspectra falls within the temperature range where lipid segregation occurs according to Fig. 9 *A*. Obviously, the ^{2}H lines are still broadened by diffusional exchange among the domains (compare to the spectrum recorded at 36.5°C). Much narrower lines were observed at lower hydration ($n_w \approx 9$), indicating that either the domain size increases or the rate of lateral water diffusion decreases (not shown).

DISCUSSION

The hydration of phosphatidylcholines has been thoroughly studied by ^{2}H-NMR spectroscopy, using the motionally averaged quadrupolar interaction of deuterium oxide (Faure et al., 1997; Finer, 1973; Finer and Darke, 1974; Gawrisch et al., 1985; Klose et al., 1992; Salsbury et al., 1972; Volke et al., 1994a,b) or by employing selectively labeled phospholipids (Bechinger and Seelig, 1991; Ulrich and Watts, 1994). However, there are still controversial subjects, e.g., the number of bound water molecules and the related area per lipid, that have only recently been critically reevaluated (Katsaras, 1998; Nagle and Tristram-Nagle, 2000). This uncertainty can be attributed to the inherent inhomogeneity of multilamellar liposomal suspensions that have been frequently used as model systems (König et al., 1997a). As shown in a recent x-ray study, the unit cell spacing increases with temperature in the liquid crystalline state of phosphatidylcholine liposomes ($n_w \geq 30$), indicating that the interbilayer space imbibes additional water from membrane defects or from the surroundings as a consequence of the onset of bilayer undulations (Costigan et al., 2000). Macroscopic alignment of multibilayers, keeping n_w slightly <30, attenuates surface undulations and ensures effective annealing of bilayer defects which justifies the notion that the entire D_2O signal reflects water that is in contact with a flat membrane interface. Hence, the average hydration per lipid n_w can be conveniently obtained by signal integration.

The small residual quadrupolar splitting, $\Delta\nu_Q^{D_2O}$, is the result of an effective motional averaging, given the large quadrupolar coupling constant of 220 kHz obtained for deuterium oxide in ice (Soda and Chiba, 1969). Nonetheless, $\Delta\nu_Q^{D_2O}$ represents an extremely sensitive and potentially useful parameter that has been previously correlated with microscopic properties of the lipid water interface (Bryant et al., 1992a,b; Gawrisch et al., 1992; Volke et al., 1994a,b). It is shown here that the motional anisotropy of the interfacial water (as deduced from $\Delta\nu_Q^{D_2O}$) reflects a uniform behavior in phosphatidylcholines that differ by as much as 46°C in their respective phase transition temperatures T_m. The temperature dependence of $\Delta\nu_Q^{D_2O}$ above T_m (Fig. 2) can be attributed to the increasing water-accessible surface area; *e.g.*, for DPPC, the area per lipid changes from 0.48 nm^2 at 20°C to 0.64 nm^2 at 50°C (Nagle and Tristram-Nagle, 2000). According to x-ray crystallography, the C=O bond of the phosphatidylcholine *sn*-2 chain is directed with its negative partial charge toward the interlamellar space (Pearson and Pascher, 1979). This results in a dipole potential that, in turn, leads to weak orientation of the water dipoles. The exposure of carbonyls increases with increasing area per lipid which further amplifies the water orientation. This simple electrostatic perspective is in agreement with a recent potential of mean force calculation which yielded a surprisingly narrow orientational distribution of water molecules at a smooth negatively charged surface (Lindahl, 2001). The orienta-

tional order parameter of interfacial water was indeed correctly reproduced in a recent molecular dynamics study of a phosphatidylcholine bilayer in the liquid crystalline state (Åman et al., 2003). Two regions along the bilayer normal with negative and positive O-H order parameters were identified, in agreement with an idea introduced in an earlier study on ion and water binding (Lindblom et al., 1976). It remains to be studied whether this sign reversal causes cancellation of the D_2O quadrupolar splittings close to the main phase transition.

An alternative interpretation invoked the Landau theory of phase transitions (Hawton and Doane, 1987; Jähnig, 1981a,b). Within this framework, Hawton and Doane derived a universal relation for the temperature dependence of $\Delta\nu_Q^{D_2O}$ obtained in oriented multilayers of saturated phospholipids, i.e., $\Delta\nu_Q^{D_2O} \propto |(T - T^*)/T|^n$, where T^* denotes the critical temperature that equals the phase transition temperature T_m for the case of a first-order transition (Hawton and Doane, 1987). Hence, the collapse of the D_2O quadrupolar splitting observed upon reaching the phase transition temperature was attributed to area fluctuations which causes fluctuating defects in the membrane-water interface where isotropic motion of the water molecules averages the residual quadrupolar interaction of the water deuterons. It must be noted, however, that this view is still controversial and that it may not be applicable to mixed bilayer systems (vide infra).

The hydration of sphingomyelins has not been studied in such detail. Only recently Jendrasiak and co-workers presented a comparative survey of binding isotherms using BET theory for a discrimination of weak and strong water adsorption (Jendrasiak and Smith, 2001). Unfortunately, measurements were performed exclusively at 22°C; i.e., the resulting isotherms corresponded to the gel state for all sphingomyelins studied. Hence, the data obtained by these authors may not be directly comparable with our results. Moreover, the hydration levels attainable by their method at a relative humidity of 100% are low—possibly a consequence of the so-called vapor pressure paradox, a phenomenon which has been recently attributed to temperature gradients within the sample volume (Katsaras, 1998).

The unusually low D_2O splitting in the liquid crystalline state of sphingomyelins may be attributed to the average orientation of the amide plane with respect to the membrane surface which involves an in-plane orientation of the C=O bond (Miller et al., 1986; Pascher, 1976; Ruocco et al., 1996). This geometry results in a small effective dipole moment of the carbonyl group (i.e., the dipole moment projected onto the bilayer normal), which excludes strong interaction with a first water layer. The small or negligible contribution of the first water layer to the overall dipole potential of the membrane interface may account for the small $\Delta\nu_Q^{D_2O}$ values in the liquid crystalline state of the sphingomyelins (Gawrisch et al., 1992). It may be further assumed that intermolecular hydrogen bonding prevents interlamellar water from entering the interfacial lipid layer. Both conditions, i.e., the average orientation of the carbonyl group and the interfacial hydrogen bond network, seem to make the sphingomyelin lipid-water interface less hydrophilic as compared to the phosphatidylcholine interface. The extent of this interfacial lipid-lipid interaction is likely to depend on the average cross-sectional area of the respective sphingomyelin. This is borne out by the observation that $\Delta\nu_Q^{D_2O}$ reaches a minimum ~3°C and 13°C $> T_m$ for BBSM and EYSM, respectively, suggesting that the area per molecule associated with these temperatures is most favorable for the H-bond network. Due to the presence of long acyl chains (45.5%, 18:0; 7.2%, 22:0; and 23.3%, 24:0; Jendrasiak and Smith, 2001), BBSM reaches the critical area close to the phase transition temperature whereas EYSM (83.9%, 16:0) needs a somewhat higher temperature.

The packing of the hydrocarbon chains in the gel state may then force the interfacial segments into a conformation with an electrostatic orientation potential that favors the alignment of water dipoles. It must be noted that Gawrisch et al. (1992) observed a significantly smaller water splitting over a large range of hydration values for DPPC than for the ether lipid dihexadecylphosphatidylcholine (DHPC), although the dipole potential for DPPC was larger by 118 mV than that of DHPC (due to the absence of the *sn*-2 carbonyl group in the ether lipid). Likewise, measurements of the dipole potential in gel state monolayers yielded smaller values for BBSM than for DPPC (328 mV vs. 575 mV; McIntosh et al., 1992) which seems to be inconsistent with the assumption of a simple relation between dipole potential and orientational ordering as measured by the D_2O quadrupolar splitting (compare to Fig. 5). A detailed analysis of bond orientations and dihedral angles will be required, e.g., by selective isotope labeling of the interfacial segments, to ascertain the conformational change that sphingomyelin undergoes during the phase transition.

The homogeneous alignment of bilayers between glass plates permits a quantitative assessment of the exchange between interlamellar deuterium oxide and labile amide and hydroxyl deuterons in the lipid-water interface. The deuteron exchange rate k_{OD} of the hydroxyl group of BBSM is ~600 s^{-1} at 45°C and $n_w = 20$, which is the same order of magnitude as the value obtained previously for the headgroup hydroxyl deuterons of POPG ($k_{OD} \approx 800\ s^{-1}$ at 30°C, $n_w = 20$; Kurze et al., 2000). This compares favorably with H_3O^+/H_2O and H_2O/OH^- hydrogen exchange rates determined for pure water (Luz and Meiboom, 1964; Meiboom, 1961), indicating that the sphingomyelin hydroxyl group has access to the interlamellar hydration layer. It may be noted, however, that the activation energies are 10 kJ/mol and 8.8 kJ/mol, respectively, for the H_3O^+ and OH^- exchange rates versus 41 kJ/mol obtained for the water-sphingomyelin deuteron exchange. A similar activation energy has been reported earlier for the proton exchange in hydrated collagen fibers (Migchelsen and Berendsen, 1973).

In sharp contrast, the amide deuteron exchange is too slow for the inversion transfer technique, suggesting that in the liquid crystalline bilayer the amide deuteron is involved in strong hydrogen bonding. These results are in agreement with the average backbone conformation derived from ^{13}C solid state NMR spectroscopy where it was shown that the sphingosine OH group is directed toward the aqueous phase (Ruocco et al., 1996). On the other hand, strong intermolecular hydrogen bonding of the sphingosine OH group has been deduced from infrared spectroscopy of BBSM bilayers in the gel state (Lamba et al., 1991). The observation that both ^{2}H signals of the labile deuterons broaden upon entering the gel phase supports the assumption of a conformational change resulting in intermolecular hydrogen bonding of the hydroxyl group, in agreement with the earlier results.

A particularly intriguing aspect of the BBSM structure is its chain length asymmetry. Binary mixtures of BBSM and POPC were studied as a paradigm for the interaction among medium chain unsaturated glycerophospholipids and sphingolipids with a long N-acyl chain, a situation prevalent in brain tissue. The phase diagram obtained by Untracht and Shipley (1977) served as a guideline that facilitated the interpretation of the present results. This phase diagram shows complete miscibility of the components above 44°C and the formation of a paratactic molecular compound at 33 mol % lecithin and 66 mol % sphingomyelin <20°C. Lateral phase separation was detected using x-ray diffraction and polarized light microscopy upon cooling below the *liquidus* line.

In the present study we have focused on the interfacial properties of the BBSM/POPC system in the physiologically relevant temperature range from 20°C to 45°C (neglecting the intermolecular compound). Considering the liquid crystalline state of the mixtures, there are two observations of interest, i.e., the acyl chain order of the selectively deuterated lecithin (POPC-d_{31}) increases and the orientational order of the interfacial water decreases with increasing BBSM concentration in the system. Specifically, the length of the so-called order parameter plateau increases, which amounts to an increasing contribution of the largest quadrupolar splitting in the ^{2}H spectrum (compare to Fig. 1). It is customary to assume that the plateau corresponds to the first methylene segments that flow from the lipid-water interface toward the bilayer center. Here we employed the *ratios* of segmental order parameters (with reference to the corresponding order parameter values of POPC alone) rather than the usual order parameter profiles (Fig. 8). The ratios are able to demonstrate the ordering effect of sphingomyelin more clearly than a direct comparison of the profiles. Thus, the overall packing density of the lipid mixture increases as a result of the presence of saturated chains, probably in combination with the capability of the sphingolipid to form interfacial hydrogen bonds. The ''condensing effect'' clearly increases with BBSM concentration while there was no indication of fluid-to-fluid demixing, in agreement with the published phase diagram (Untracht and Shipley, 1977). An analogous behavior has been recently reported for mixtures containing a ceramide (<20 mol %) and POPC where both components were selectively deuterated (Hsueh et al., 2002). It may be noted, however, that in the POPC/ceramide system a metastable solid phase appears when the ceramide content exceeds 20 mol %.

Increasing the mole fraction of sphingomyelin in the mixture also reduces the ordering of interfacial water, probably as a result of the diminished fraction of water molecules in the carbonyl region of the bilayer. Reduced spontaneous transbilayer diffusion of glucose has been observed earlier as a further consequence of the condensing effect of sphingomyelin in mixed phospholipid membranes (Hertz and Barenholz, 1975). It can be also assumed that the presence of sphingomyelin modulates the interaction of amphiphilic peptides and proteins with the membrane interface.

The onset and completion of the phase transition in the 2:1 BBSM/POPC-d_{31} mixture is reflected by the ^{2}H quadrupolar splittings of the deuterated POPC alkyl chain which can be most easily recognized by the splittings arising from the terminal methyl group at reduced interlamellar hydration (Fig. 9 *A*). The observation of a single ^{2}H doublet over the temperature range of the transition indicates that almost pure BBSM gel state domains grow out of the mixture when the system crosses the *liquidus* line. This again suggests that the phase behavior of the BBSM/POPC mixture differs from that of the system ceramide/POPC where a mixed ceramide/POPC gel phase was found below the *liquidus* line (Hsueh et al., 2002).

Surface domains may also account for the observation of D_2O subspectra over the temperature range where phase separation occurs (Fig. 9 *B*). Such domains have to be sufficiently large so as to preclude signal averaging by random lateral motion of the interlamellar D_2O. An order-of-magnitude estimate of the domain size can be made, based on the diffusion equation in two dimensions. Using the diffusion constant for lateral interlamellar water motion of $2.5 \times 10^{-10} m^2 s^{-1}$ obtained at the same temperature and hydration in egg phosphatidylcholine (Wassall, 1996), and taking account of the frequency separation of the coexisting D_2O signals, this calculation yields a minimum domain area required for the observation of separate water spectra of 6 μm^2. This is well within the range of domain sizes determined by epifluorescence microscopy in monolayers of phospholipid/cholesterol or sphingomyelin/cholesterol mixtures (Dietrich et al., 2001; Radhakrishnan et al., 2000).

This work was supported by the Deutsche Forschungsgemeinschaft, grant BE 828/8.

REFERENCES

Åman, K., E. Lindahl, O. Edholm, P. Hakansson, and P. O. Westlund. 2003. Structure and dynamics of interfacial water in an L α phase lipid bilayer from molecular dynamics simulations. *Biophys. J.* 84:102–115.

Anderson, R. G., and K. Jacobson. 2002. A role for lipid shells in targeting proteins to caveolae, rafts, and other lipid domains. *Science*. 296:1821–1825.

Barenholz, Y. 1984. Sphingomyelin-lecithin balance in membranes: composition, structure, and function relationships. *In* Physiology of Membrane Fluidity. M. Shinitzky, editor. CRC Press, Boca Raton, FL. pp.131–73.

Barenholz, Y., and T. E. Thompson. 1999. Sphingomyelin: biophysical aspects. *Chem. Phys. Lipids*. 102:29–34.

Bechinger, B., and J. Seelig. 1991. Conformational changes of the phosphatidylcholine headgroup due to membrane dehydration. A ^{2}H-NMR study. *Chem. Phys. Lipids*. 58:1–5.

Bruzik, K. S. 1988. Conformation of the polar headgroup of sphingomyelin and its analogues. *Biochim. Biophys. Acta*. 939:315–326.

Bryant, G., J. M. Pope, and J. Wolfe. 1992a. Low hydration phase properties of phospholipid mixtures. Evidence for dehydration-induced fluid-fluid separations. *Eur. Biophys. J*. 21:223–232.

Bryant, G., J. M. Pope, and J. Wolfe. 1992b. Motional narrowing of the ^{2}H NMR spectra near the chain melting transition of phospholipid/D_2O mixtures. *Eur. Biophys. J*. 21:363–367.

Calhoun, W. I., and G. G. Shipley. 1979. Fatty acid composition and thermal behavior of natural sphingomyelins. *Biochim. Biophys. Acta*. 555:436–441.

Costigan, S. C., P. J. Booth, and R. H. Templer. 2000. Estimations of lipid bilayer geometry in fluid lamellar phases. *Biochim. Biophys. Acta*. 1468:41–54.

Davis, J. H., K. R. Jeffrey, M. Bloom, and M. I. Valic. 1976. Quadrupolar echo deuteron magnetic resonance spectroscopy in ordered hydrocarbon chains. *Chem. Phys. Lett*. 42:390–394.

Dietrich, C., L. A. Bagatolli, Z. N. Volovyk, N. L. Thompson, M. Levi, K. Jacobson, and E. Gratton. 2001. Lipid rafts reconstituted in model membranes. *Biophys. J*. 80:1417–1428.

Faure, C., L. Bonakdar, and E. J. Dufourc. 1997. Determination of DMPC hydration in the L_a and $L_{b'}$ phases by ^{2}H solid state NMR of D_2O. *FEBS Lett*. 405:263–266.

Finer, E. G. 1973. Interpretation of deuteron magnetic resonance spectroscopic studies of the hydration of macromolecules. *J. Chem. Soc. Faraday Trans*. 69:1590–1600.

Finer, E. G., and A. Darke. 1974. Phospholipid hydration studied by deuteron magnetic resonance spectroscopy. *Chem. Phys. Lipids*. 12:1–16.

Florin-Christensen, J., C. E. Suarez, M. Florin-Christensen, M. Wainszelbaum, W. C. Brown, T. F. McElwain, and G. H. Palmer. 2001. A unique phospholipid organization in bovine erythrocyte membranes. *Proc. Natl. Acad. Sci. USA*. 98:7736–7741.

Gawrisch, K., W. Richter, A. Möps, P. Balgavy, K. Arnold, and G. Klose. 1985. The influence of water concentration on the structure of egg yolk phospholipid/water dispersions. *Stud. Biophys*. 108:5–16.

Gawrisch, K., D. Ruston, J. Zimmerberg, V. A. Parsegian, R. P. Rand, and N. Fuller. 1992. Membrane dipole potentials, hydration forces, and the ordering of water at membrane surfaces. *Biophys. J*. 61:1213–1223.

Hawton, M. H., and J. W. Doane. 1987. Pretransitional phenomena in phospholipid/water multilayers. *Biophys. J*. 52:401–404.

Hertz, R., and Y. Barenholz. 1975. Permeability and integrity properties of lecithin-sphingomyelin liposomes. *Chem. Phys. Lipids*. 15:138–156.

Hsueh, Y.-W., R. Giles, N. Kitson, and J. Thewalt. 2002. The effect of ceramide on phosphatidylcholine membranes: a deuterium NMR study. *Biophys. J*. 82:3089–3095.

Hübner, W., and A. Blume. 1998. Interactions at the lipid-water interface. *Chem. Phys. Lipids*. 96:99–123.

Jähnig, F. 1981a. Critical effects from lipid-protein interaction in membranes. I. Theoretical description. *Biophys. J*. 36:329–345.

Jähnig, F. 1981b. Critical effects from lipid-protein interaction in membranes. II Interpretation of experimental results. *Biophys. J*. 36: 347–357.

Jendrasiak, G. L., and R. L. Smith. 2001. The effect of the choline head group on phospholipid hydration. *Chem. Phys. Lipids*. 113:55–66.

Katsaras, J. 1998. Adsorbed to a rigid substrate, dimyristoylphosphatidylcholine multibilayers attain full hydration in all mesophases. *Biophys. J*. 75:2157–2162.

Klose, G., B. König, and F. Paltauf. 1992. Sorption isotherms and swelling of POPC in H_2O and ^2H_2O. *Chem. Phys. Lipids*. 61:265–270.

König, B., U. Dietrich, and G. Klose. 1997a. Hydration and structural properties of mixed lipid/surfactant model membranes. *Langmuir*. 13: 525–532.

König, B. W., H. H. Strey, and K. Gawrisch. 1997b. Membrane lateral compressibility determined by NMR and x-ray diffraction: effect of acyl chain polyunsaturation. *Biophys. J*. 73:1954–1966.

Kurze, V., B. Steinbauer, T. Huber, and K. Beyer. 2000. A ^{2}H NMR study of macroscopically aligned bilayer membranes containing interfacial hydroxyl residues. *Biophys. J*. 78:2441–2451.

Lamba, O. P., D. Borchman, S. K. Sinha, S. Lal, M. C. Yappert, and M. F. Lou. 1991. Structure and molecular conformation of anhydrous and of aqueous sphingomyelin bilayers determined by infrared and Raman spectroscopy. *J. Mol. Struct*. 248:1–24.

Led, J. J., and H. Gesmar. 1982. The applicability of the magnetization-transfer NMR technique to determine chemical exchange rates in extreme cases. The importance of complementary experiments. *J. Magn. Reson*. 49:444–463.

Li, X. M., M. M. Momsen, J. M. Smaby, H. L. Brockman, and R. E. Brown. 2001. Cholesterol decreases the interfacial elasticity and detergent solubility of sphingomyelins. *Biochemistry*. 40:5954–5963.

Lindahl, E. 2001. Computational Modeling of Biological Membrane and Interface Dynamics. Royal Institute of Technology, Stockholm, Sweden. (PhD thesis.)

Lindblom, G., N. O. Persson, and G. Arvidson. 1976. Ion binding and water orientation in lipid model membrane systems studied by NMR. *Adv. Chem. Ser*. 152:121–141.

London, E., and D. A. Brown. 2000. Insolubility of lipids in Triton X-100: physical origin and relationship to sphingolipid/cholesterol membrane domains (rafts). *Biochim. Biophys. Acta*. 1508:182–195.

Luz, Z., and S. Meiboom. 1964. The activation energies of proton transfer reactions in water. *J. Am. Chem. Soc*. 86:4768–4769.

Mahfoud, R., N. Garmy, M. Maresca, N. Yahi, A. Puigserver, and J. Fantini. 2002. Identification of a common sphingolipid-binding domain in Alzheimer, prion, and HIV-1 proteins. *J. Biol. Chem*. 277:11292–11296.

McIntosh, T. J., S. A. Simon, D. Needham, and C. H. Huang. 1992. Interbilayer interactions between sphingomyelin and sphingomyelin/cholesterol bilayers. *Biochemistry*. 31:2020–2024.

Meiboom, S. 1961. Nuclear magnetic resonance study of the proton transfer in water. *J. Chem. Phys*. 34:375–388.

Migchelsen, C., and H. J. C. Berendsen. 1973. Proton exchange and molecular orientation of water in hydrated collagen fibers. An NMR study of H2O and D2O. *J. Chem. Phys*. 59:296–305.

Miller, I. R., D. Chapman, and A. F. Drake. 1986. Circular dichroism spectra of aqueous dispersions of sphingolipids. *Biochim. Biophys. Acta*. 856:654–660.

Nagle, J. F., Y. Liu, S. Tristram-Nagle, R. M. Epand, and R. E. Stark. 1999. Re-analysis of magic angle spinning nuclear magnetic resonance determination of interlamellar waters in lipid bilayer dispersions. *Biophys. J*. 77:2062–2065.

Nagle, J. F., and S. Tristram-Nagle. 2000. Structure of lipid bilayers. *Biochim. Biophys. Acta*. 1469:159–195.

Naslavsky, N., H. Shmeeda, G. Friedlander, A. Yanai, A. H. Futerman, Y. Barenholz, and A. Taraboulos. 1999. Sphingolipid depletion increases formation of the scrapie prion protein in neuroblastoma cells infected with prions. *J. Biol. Chem*. 274:20763–20771.

Nyberg, L., R. D. Duan, and A. Nilsson. 1998. Sphingomyelin. A dietary component with structural and biological function. *Prog. Coll. Polym. Sci*. 108:119–128.

Pascher, I. 1976. Molecular arrangements in sphingolipids. Conformation and hydrogen bonding of ceramide and their implication on membrane stability and permeability. *Biochim. Biophys. Acta.* 455:433–451.

Pearson, R. H., and I. Pascher. 1979. The molecular structure of lecithin dihydrate. *Nature.* 281:499–501.

Pettegrew, J. W., K. Panchalingam, R. L. Hamilton, and R. J. McClure. 2001. Brain membrane phospholipid alterations in Alzheimer's disease. *Neurochem. Res.* 26:771–782.

Prosser, R. S., S. I. Daleman, and J. H. Davis. 1994. The structure of an integral membrane peptide: a deuterium NMR study of gramicidin. *Biophys. J.* 66:1415–1428.

Radhakrishnan, A., T. G. Anderson, and H. M. McConnell. 2000. Condensed complexes, rafts, and the chemical activity of cholesterol in membranes. *Proc. Natl. Acad. Sci. USA.* 97:12422–12427.

Ruocco, M. J., D. J. Siminovitch, J. R. Long, S. K. Das Gupta, and R. G. Griffin. 1996. ^{2}H and ^{13}C nuclear magnetic resonance study of *n*-palmitoylgalactosylsphingosine (cerebroside)/cholesterol bilayers. *Biophys. J.* 71:1776–1788.

Salmon, A., S. W. Dodd, G. D. Williams, J. M. Beach, and M. F. Brown. 1987. Configurational statistics of acyl chains in polyunsaturated lipid bilayers from ^{2}H NMR. *J. Am. Chem. Soc.* 109:2600–2609.

Salsbury, N. J., A. Darke, and D. Chapman. 1972. Deuteron magnetic resonance studies of water associated with phospholipids. *Chem. Phys. Lipids.* 8:142–151.

Schindler, H., and J. Seelig. 1975. Deuterium order parameters in relation to thermodynamic properties of a phospholipid bilayer. *Biochemistry.* 14:2283–2287.

Schmidt, C. F., Y. Barenholz, and T. E. Thompson. 1977. A nuclear magnetic resonance study of sphingomyelin in bilayer systems. *Biochemistry.* 16:2649–2656.

Siminovitch, D. J., and K. R. Jeffrey. 1981. Orientational order in the choline headgroup of sphingomyelin: a ^{14}N-NMR study. *Biochim. Biophys. Acta.* 645:270–08.

Soda, G., and T. Chiba. 1969. Deuterium magnetic resonance study of cupric sulfate pentahydrate. *J. Chem. Phys.* 50:439–455.

Talbott, C. M., I. Vorobyov, D. Borchman, K. G. Taylor, D. B. DuPre, and M. C. Yappert. 2000. Conformational studies of sphingolipids by NMR spectroscopy. II. Sphingomyelin. *Biochim. Biophys. Acta.* 1467:326–337.

Ulrich, A. S., and A. Watts. 1994. Molecular response of the lipid headgroup to bilayer hydration monitored by ^{2}H-NMR. *Biophys. J.* 66: 1441–1449.

Untracht, S. H., and G. G. Shipley. 1977. Molecular interactions between lecithin and sphingomyelin. Temperature- and composition-dependent phase separation. *J. Biol. Chem.* 252:4449–4457.

Villalain, J., A. Ortiz, and J. C. Gomez-Fernandez. 1988. Molecular interactions between sphingomyelin and phosphatidylcholine in phospholipid vesicles. *Biochim. Biophys. Acta.* 941:55–62.

Vist, M. R., and J. H. Davis. 1990. Phase equilibria of cholesterol/dipalmitoylphosphatidylcholine mixtures: ^{2}H nuclear magnetic resonance and differential scanning calorimetry. *Biochemistry.* 29:451–464.

Volke, F., S. Eisenblätter, J. Galle, and G. Klose. 1994a. Dynamic properties of water at phosphatidylcholine lipid-bilayer surfaces as seen by deuterium and pulsed field gradient proton NMR. *Chem. Phys. Lipids.* 70:121–131.

Volke, F., S. Eisenblätter, and G. Klose. 1994b. Hydration force parameters of phosphatidylcholine lipid bilayer as determined from ^{2}H-NMR studies of deuterated water. *Biophys. J.* 67:1882–1887.

Wassall, S. R. 1996. Pulsed field gradient-spin echo NMR studies of water diffusion in a phospholipid model membrane. *Biophys. J.* 71:2724–2732.

Yorek, M. A. 1993. Biological distribution. *In* Phospholipids Handbook. G. Cevc, editor. Marcel Dekker, New York. pp.745–775.